Concerning the Participation of the Anthracene/*N,N*-Dimethylaniline Exciplex in Anthracene Photodimerization[1a,b]

Jack Saltiel,*[1c] David E. Townsend,[1c] Brant D. Watson,[1d] Patrick Shannon,[1c,d] and Stephen L. Finson[1c]

Contribution from the Department of Chemistry and the Institute of Molecular Biophysics, Florida State University, Tallahassee, Florida 32306.
Received July 2, 1976

Abstract: Steady-state and transient fluorescence measurements have been made using mixtures of anthracene and *N,N*-dimethylaniline in benzene. These measurements show that the exciplex lifetime is shortened as the *N,N*-dimethylaniline concentration is increased, possibly due to the formation of a triplex. The exciplex lifetime is independent of anthracene concentration for [A] $\leq$ 0.03 M, but decreases at high anthracene concentration. A study of anthracene photodimerization suggests that the exciplex or a higher excited aggregate participates in this reaction at high anthracene concentration and that the presence of oxygen enhances dianthracene yields. Rate constants for several of the photophysical and photochemical processes are reported.

Kinetic observations have led to the suggestion that an anthracene/*trans,trans*-2,4-hexadiene singlet exciplex functions as an intermediate in anthracene photodimerization.[2,3] Since emission spectroscopy is not easily applicable to a study of this exciplex,[4] it was of interest to note results of earlier studies showing that anthracene photodimer forms in high yield when anthracene, A, is irradiated in the presence of *N,N*-dimethylaniline, DMA.[5,6] The presence of well-characterized exciplex emissions in A/DMA[7] and A/*N,N*-diethylaniline[8-10] systems prompted this study of the role of A/DMA exciplexes in anthracene photodimerization.[11]

Results

Steady-State Measurements. The quenching of A fluorescence by DMA in benzene was determined at 23.2 °C by measuring emission intensity at 384 nm as a function of DMA concentration both in degassed, I_{deg}, and air-saturated solutions, I_{ox}. I_0/I ratios are shown in Table I. Concomitant with the quenching of A fluorescence is the appearance of a greenish, broad, structureless A/DMA exciplex emission, λ_{max} $\sim$ 508 nm. As a measure of this emission Table I gives the relative fluorescence intensity at 500 nm in degassed and air-saturated solutions. Representative emission spectra corrected for nonlinearity of instrumental response are shown in Figure 1. Relative areas of such spectra were determined by cutting and weighing Xerox copies of larger versions of these spectra. The relative weights were converted to total fluorescence quantum yields, ϕ_f, Table II, by assuming that the fluorescence quantum yield of anthracene at low anthracene concentrations is 0.27.[13-16] Since the exciplex does not emit at 384 nm the I_0/I values in Table I give anthracene fluorescence quantum yields, ϕ_{fm}, which when subtracted from the total fluorescence quantum yields give the exciplex fluorescence quantum yields, ϕ_{fe}, shown in Table II. As expected ϕ_{fe} values are in good agreement with the relative emission intensities measured at 500 nm (Table I). The quenching effect at the highest DMA concentrations employed is augmented due to competition by DMA for the exciting light, as indicated by UV absorption spectra showing that the optical density at 352 nm of a 6.7×10^{-5} M air-saturated anthracene solution in benzene increases from 0.226 to 0.308 (1-cm path) when the solution is made 0.986 M in DMA. The DMA solution also shows a weak absorption tail which extends well into the visible, optical density 0.03 at 420 nm. Since upon admission of air DMA solutions turn from colorless to yellow, the change being reversible, DMA absorption is expected to interfere less in degassed solutions. Nonetheless, the emission spectra of the degassed 0.986 M DMA solutions described in Tables I and II and Figure 1 show a weak higher energy emission ($\sim$1% of total area) which is absent in the other spectra and may be coming from excited DMA molecules.

Lifetime Measurements. Decay profiles of A fluorescence were obtained by monitoring the emission at 427 nm of degassed solutions of A and DMA in benzene at 25 °C. Experimental procedure 1 (see Experimental Section) was employed. First-order decay plots were linear until the signal intensity had dropped to less than 5% of its maximum value. Especially for the samples containing the higher DMA concentrations a small long-lived emission component was easily discernible. A typical decay curve is shown in Figure 2. This component was absent in the anthracene sample which contained no DMA. More prominent slow decay components have been observed from A/DMA solutions in cyclohexane.[17] Detailed kinetic analysis has shown these to be due to fluorescence from ^{1}A* generated by exciplex dissociation.[17] The first-order decay constants and estimated uncertainties shown in Table III were obtained by treating only the fast component portions of the fluorescence decay. An approximate treatment of the delayed component will be presented in the Discussion.

A/DMA exciplex decay rate constants were obtained by monitoring the emission at 500 nm of degassed solutions of A and DMA in benzene at 23 °C. Unless otherwise indicated, experimental procedure 2 was employed. First-order exciplex decay rate constants obtained at different DMA concentrations and a constant A concentration of 5.0×10^{-5} M are shown in Table IV. First-order exciplex decay rate constants obtained at different A concentrations and constant DMA concentrations of 0.0395 and 0.986 M are presented in Table V. No significant deviations from single exponential decay were noted in exciplex emission, but in all cases only the decaying portions of the kinetic curves were employed in determining the rate constants.

Photochemical Measurements. Anthracene disappearance yields were determined as a function of A and DMA concentration in benzene. Excitation was at 366 nm. The benzophenone, 0.05 M, sensitized photoisomerizations of *cis*-1,3-pentadiene,[18,19] and *trans*-stilbene[20,21] were used for actinometry. Anthracene disappearance yields and actinometry conversions are shown in Tables VI and VII. Several sets of irradiations were also carried out at 30 °C (procedure 1) in which relative anthracene disappearance yields were obtained in the presence and in the absence of DMA. The results were generally in

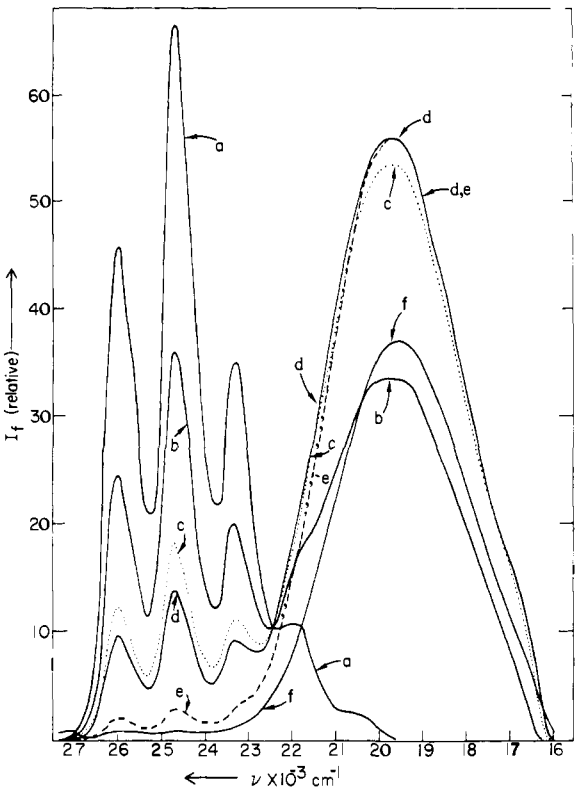

Figure 1. Corrected emission spectra of 5.0×10^{-5} M A benzene solutions and the following DMA concentrations: (a) none; (b) 0.0197 M; (c) 0.0592 M; (d) 0.0789 M; (e) 0.316 M; (f) 0.986 M.

Table I. Dependence of A and A/DMA Fluorescence Intensity on DMA Concentration

	384 nm		500 nm	
[DMA], M	I_0/I^a	$I_0/I_{ox}{}^b$	I^a	$I_{deg}/I_{ox}{}^c$
0	1.00	1.19	0.30	1.19
0.0197	1.8_4	2.1_2	10.7	6.2_0
0.0395	2.7_8	3.0_3	$15._0$	6.4_2
0.0592	3.6_4	4.1_4	$16._4$	6.3_7
0.0789	5.0_6	5.2_1	$17._3$	6.3_2
0.0789	4.7_4	5.2_1	$17._4$	6.4_1
0.118	7.2	8.2	$17._6$	6.2_6
0.158	$10._0$	$10._6$	$18._6$	6.3_3
0.197	$12._2$	$13._8$	$18._1$	5.9_7
0.237	$15._5$	$17._4$	$18._3$	5.8_7
0.316	$24._2$	$28._7$	$17._4$	5.7_3
0.395	$33._8$	$35._4$	$17._3$	5.0_4
0.986	~260.		$12._4$	
0.986	~250.		$11._4$	

[a] Degassed solutions, [A] = 5.0×10^{-5} M, excitation wavelength 352 nm. [b] As in *a* but air-saturated solutions. [c] The effect of air saturation for each DMA concentration.

agreement with those in Tables VI and VII. They will not be reported, since the anthracene losses were high, cf., however, footnote 73. It should be noted that in duplicate determinations using procedure 1 much better precision was generally achieved with samples containing DMA. The effect of oxygen on the relative yield of anthracene disappearance in the presence of DMA was determined by parallel irradiation of degassed and air-saturated samples of identical solutions, Table VIII.

An anthracene solution, 5.0×10^{-3} M, 100 ml, containing 1.0 M DMA was irradiated (366 nm), while a constant stream of nitrogen was bubbled through it. The irradiation was

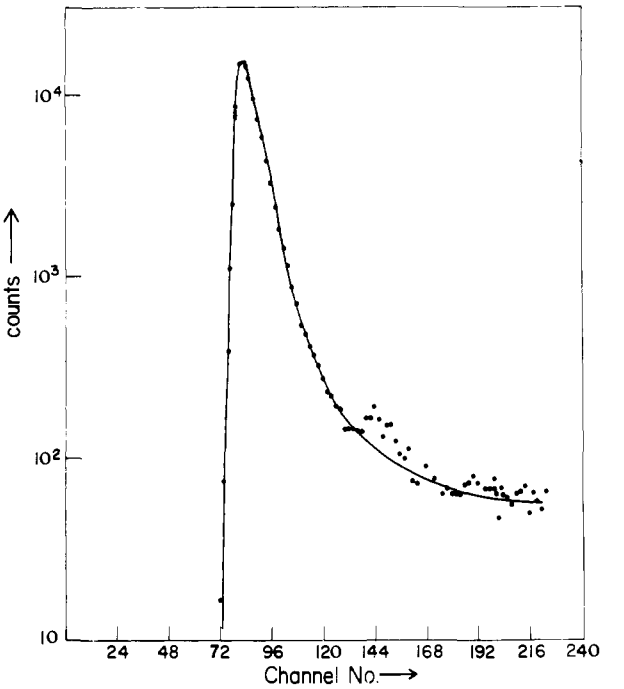

Figure 2. Typical decay curve of A fluorescence, 427 nm, in the presence of DMA, seventh entry in Table III, 3.21 ch/ns.

Table II. Fluorescence Quantum Yields in the System A/DMA in Benzene[a]

[DMA], M	$\phi_f{}^b$	$\phi_{fm}{}^c$	ϕ_{fc}
0	0.27	0.27	0
0.0197	0.38_5	0.14_7	0.23_8
0.0395	0.35_3	0.09_6	0.25_7
0.0592	0.43_8	0.07_4	0.36_4
0.0789	0.41_5	0.05_7	0.35_8
0.0789	0.43_4	0.05_8	0.37_6
0.118	0.42_6	0.03_7	0.38_9
0.158	0.42_0	0.02_9	0.39_1
0.197	0.42_6	0.02_2	0.40_4
0.237	0.43_8	0.01_9	0.41_9
0.316	0.39_7	0.01_3	0.38_4
0.395	0.36_5	0.01_0	0.35_5
0.986	0.24_9	~0.001	0.24_7
0.986	0.22_8	~0.001	0.22_6

[a] Degassed solutions described in Table I. [b] Based on $\phi_{fm} = 0.27$ for anthracene, see text. [c] Based on I_0/I values at 384 nm in Table I.

stopped when the strong green fluorescence had visibly become a lighter green. The solvent was removed by rotary evaporation and the DMA by warming to 45–50 °C under vacuum. A TLC on silica gel plates, developed with cyclohexane containing a few drops of ammonium hydroxide showed the presence of at least five products in addition to a small spot corresponding to unreacted anthracene. A few white crystals were isolated from the residue and shown to be dianthracene (identical IR with that of an authentic sample). The filtered residue was dissolved in CCl_4 and basic components were extracted by three washings with 5% HCl. The aqueous fraction was made basic with KOH and extracted with benzene. After drying and removal of solvent, TLC's were run as above on the neutral and basic residues obtained. Spots with R_f value close to that of anthracene were noted for both residues. There were two additional spots in the TLC of the basic residue and three additional spots in the TLC of the neutral residue; all these spots were present in the TLC of the residue prior to HCl extraction

Table III. Decay Rate Constants of A Singlets as a Function of DMA Concentration[a]

[DMA], M × 10³	k_{obsd}, $s^{-1} \times 10^{-8}$
0	2.26 ± 0.04
2.47	2.58 ± 0.07
4.93	2.87 ± 0.08
9.86	3.28 ± 0.08
12.3	3.39 ± 0.09
14.8	3.73 ± 0.10
19.7	4.24 ± 0.12
22.2	4.35 ± 0.14
24.7	4.59 ± 0.16

[a] [A] = 6.7×10^{-5} M in benzene.

Table IV. A/DMA Exciplex Decay Rate Constants as a Function of DMA Concentration[a]

[DMA], M	k_{obsd}, $s^{-1} \times 10^{-7}$
0.0079	0.84 ± 0.04
0.0197	0.86 ± 0.04
0.0395	0.93 ± 0.04
0.0395	0.81 ± 0.04[b]
0.0789	0.81 ± 0.04
0.158	0.89 ± 0.04
0.197	0.89 ± 0.04
0.395	1.02 ± 0.04
0.592	1.09 ± 0.04
0.986	1.25 ± 0.04

[a] [A] = 5.0×10^{-5} M in benzene. [b] [A] = 1.0×10^{-5} M in benzene.

Table V. A/DMA Exciplex Decay Rate Constants as a Function of A Concentration

[A], M × 10³	k_{obsd},[a] $s^{-1} \times 10^{-7}$	k_{obsd},[b] $s^{-1} \times 10^{-7}$
0.050	1.23 ± 0.04	0.95 ± 0.04
0.100	1.21 ± 0.04	0.93 ± 0.04
0.300	1.29 ± 0.04	
0.500		1.00 ± 0.04
1.00	1.25 ± 0.04	
2.00	1.21 ± 0.04	1.01 ± 0.04
3.00	1.19 ± 0.04	0.92 ± 0.04
4.00	1.27 ± 0.04	0.96 ± 0.04
5.00	1.29 ± 0.04	
5.05	1.26 ± 0.02[c]	
6.00	1.26 ± 0.04	
7.00	1.25 ± 0.04	
30	1.29 ± 0.02[c]	
30	1.31 ± 0.05[d]	
	5.6 ± 0.10[d,e]	
60	1.32 ± 0.05	
70	1.34 ± 0.02[c]	
90	1.56 ± 0.10[d]	
	5.6 ± 0.10[d,e]	
~100	1.46 ± 0.02[c]	

[a] [DMA] = 0.986 M in benzene. [b] [DMA] = 0.0395 M in benzene. [c] Experimental procedure 1. [d] Experimental procedure 3. [e] In the presence of air.

and had smaller R_f values than anthracene. The identity of these products was not determined.

Dianthracene, A_2, yields were determined gravimetrically for several A and DMA concentrations. The results are shown in Table IX. The solubility of dianthracene in benzene was found to be 0.19 mg/ml at room temperature. In some instances (i.e., dilute A, low conversion) it was necessary to concentrate solutions in order to induce dimer precipitation. The anthracene loss was not determined in initial experiments for which "large" is entered in the appropriate column. Solutions for these runs were irradiated until the green emission

Table VI. Anthracene Disappearance Yields in the Absence of DMA, 366 nm[a]

Degassed, 22.4 °C[b]		Air, 23.2 °C[c]	
$[A]_0$, M × 10²	%A lost	$[A]_0$, M × 10²	%A lost
0.50_5	22.6	0.50_0	22.1
0.83_3	20.1	0.75_0	21.5
1.01	17.8	1.00	20.4
1.25	18.4	1.50	18.3
2.02	16.7	2.00	17.6
4.17	10.8	3.00	15.6
5.05	10.2	5.00	12.1

[a] Irradiation procedure 2. [b] Actinometry, *trans*-stilbene, 0.050_2 M, 16.7% conversion; corrected conversion[18] 19.5%. [c] Actinometry, *trans*-stilbene, 0.050_3 M, 20.2% conversion; corrected conversion[18] 24.7%.

Table VII. Anthracene Disappearance Yields in the Presence of DMA, 366 nm[a]

$[A]_0$, M × 10²	[DMA], M × 10²	%A lost	Actinometry,[b] M, %
0.72_6	3.94	8.0	0.0799, 6.79
1.33	3.94	11.7	0.0799, 14.82
2.53	3.94	11.4	0.0799, 14.82
3.61	3.94	7.7	0.0799, 9.33
4.75	3.94	9.5	0.0986, 11.76
4.81	3.94	6.3	0.0799, 9.33
6.03	3.94	8.8	0.0986, 11.76
7.50	3.94	7.9	0.0986, 11.76
0.30_0	98.4	33.6	0.100, 2.90
0.60_1	98.4	16.8	0.100, 2.90
1.20	98.4	17.4	0.100, 5.97
2.40	98.4	8.9	0.100, 5.97
3.61	98.4	10.8	0.100, 9.03
4.00	98.4	17.0	0.0772, 19.28
4.81	98.4	8.6	0.100, 9.03
3.03	98.4	6.3	0.091, 4.96
5.99	98.4	8.2	0.091, 12.51
8.26	98.4	6.4	0.091, 12.51

[a] Degassed solutions, irradiation procedure 2, 23 ± 1 °C, used throughout except for last three entries where procedure 1 was used, 30 °C. [b] *trans*-Stilbene actinometry except for last three entries where *cis*-1,3-pentadiene was used; numbers are initial olefin concentration and corrected conversion.

Table VIII. The Effect of Oxygen on the Efficiency of Anthracene Disappearance, 366 nm, 30 °C[a]

		%A lost	
[A], × 10²	[DMA], × 10²	Degassed	Air
0.060	98.6	18.9	4.8
0.060	98.6	14.1	4.4
0.073	98.6	6.3	1.6_6
0.40	98.6	27.8	8.1

[a] Irradiation procedure 1.

Table IX. Anthracene Dimer Yields in the Presence of DMA

[A], × 10^2	[DMA], × 10^2	%A lost[a]	%A_2 formed[b]	Conditions
0.099_9	3.94	21.0	8.4 ± 0.8	25 °C, N_2, uranium filter
1.01	3.94	25.0	66.3 ± 3.2	25 °C, 366 nm, degassed
2.99	3.94	23.8	91.2 ± 2.5	25 °C, 366 nm, degassed
5.51	3.94	38.1	97.0 ± 1.0	25 °C, 366 nm, degassed
7.53	3.94	31.3	98.1 ± 1.0	25 °C, 366 nm, degassed
3.08	98.4	25.8	14.4 ± 0.4	25 °C, 366 nm, degassed
4.99	98.4	23.1	28.2 ± 0.4	25 °C, 366 nm, degassed
7.00	98.4	16.8	43.6 ± 1.0	25 °C, 366 nm, degassed
8.22	98.4	8.9	56.1 ± 2.8	25 °C, 366 nm, degassed
8.52	98.4	11.1	47.1 ± 1.7[c]	25 °C, 366 nm, degassed
8.98	98.6	29.4	72.9 ± 2.3	30 °C, 366 nm, air
10	98.6	large	23.0	366 nm, degassed
10	98.6	large	31.3[d]	Pyrex filter, N_2
10	98.6	large	35.3[e]	Pyrex filter, N_2
10	98.6	large	47.3[d]	Pyrex filter, air
10	98.6	large	60.9[e]	Pyrex filter, air

[a] Determined by UV. [b] Minimum yields, uncertainties based on maximum errors of ±0.2 mg in weights and ±0.002 units in absorbances. [c] This sample was prepared by removing the dimer and replenishing the anthracene lost in the preceding run. [d] Irradiated in parallel, 5-ml samples. [e] As in *d*, but 3-ml samples.

became very weak. It was later found that samples in which anthracene is almost completely destroyed still show strong green emission. In the later determinations the A_2 yields were also corrected for small amounts of A which coprecipitate with the dimer. This was done by extracting the precipitates with a known quantity of benzene and determining the concentration of anthracene from the UV absorbance of the solution. A serious attempt was made to develop an IR analysis procedure for determining A/A_2 ratios in small (3–4 ml) samples, which were irradiated to lower conversions than those in Table IX. Generally, the results from these experiments are consistent with those shown in Table IX, but are not reported owing to the low precision achieved.

Discussion

Irradiation of benzene solutions of A in the presence of DMA (1 M) has been reported to yield dimer (90% yield) when high A concentrations (~0.1 M) are employed, while in acetonitrile 9-(*p*-dimethylaminophenyl)-9,10-dihydroanthracene (60–65% yield), 9,10-dihydroanthracene (5–10% yield) and 9,9′-bianthryl (10–20% yield) are the major photoproducts.[5,6] There is also a report that DMA (0.015 M) suppresses the photodimerization of A (0.02 M) in benzene by 28%.[22] Anthracene dimer formation in the presence of DMA was at first assumed to take the normal photodimerization pathway via anthracene excimers, $^1(AA)^*$,[5,6,23] but it was later reasoned that it could involve interaction between the A/DMA exciplex and a ground state anthracene molecule.[24] It was suggested that in acetonitrile this dimerization mechanism is suppressed, since in the more polar solvent rapid electron transfer in the exciplex gives ion radicals which serve as precursors to the other photoproducts.[24] In fact, ion radical formation in acetonitrile may proceed directly without the intervening formation of the exciplex,[23-29] thus precluding quencher-catalyzed[2] photodimer formation in this solvent.

The spectroscopic and photochemical observations obtained in this work better characterize the formation and behavior of A/DMA exciplexes in benzene and test their possible participation in anthracene photodimerization.

Spectroscopic Observations. The Stern–Volmer plot of the anthracene (384 nm) I_0/I data in Table I shows marked upward curvature at [DMA] > 0.06 M, Figure 3. A detailed analysis of the kinetics of monomer and exciplex fluorescence for the A/DMA system in cyclohexane, [DMA] ≤ 0.1 M, strongly suggests that a small upward curvature in that concentration range is accounted for by including the time dependence of the rate constant for exciplex formation, k_e, in the mechanism.[17] This time dependence is due to transient diffusional gradients, which though usually neglected, can be important in diffusion-controlled reactions.[17] The very pronounced curvature which we observe at higher concentrations is probably due mainly to either of two static quenching mechanisms. The first involves instantaneous quenching of excited A singlets, $^1A^*$, by a DMA molecule already present within a critical interaction volume ("active sphere" model[30]) and the second involves formation of a ground state A/DMA complex which allows direct excitation of A molecules already associated with a DMA molecule.[31-33] Assuming for the moment that the $^1A^*$/DMA reaction is diffusion controlled, the active sphere mechanism is expected to contribute at [DMA] > 0.1 M, since only in that concentration region would a significant number of $^1A^*$ molecules be expected to form in the presence of a randomly distributed DMA nearest neighbor molecule.[34] Since the curvature in Figure 3 becomes apparent very close to this concentration limit, no clear preference for either static mechanism is indicated by these data.[35] For the purpose of this discussion the mechanism in eq 1–6 will be employed, which arbitrarily assigns all the curvature in Figure 3 to ground-state complex formation, eq 1.[35]

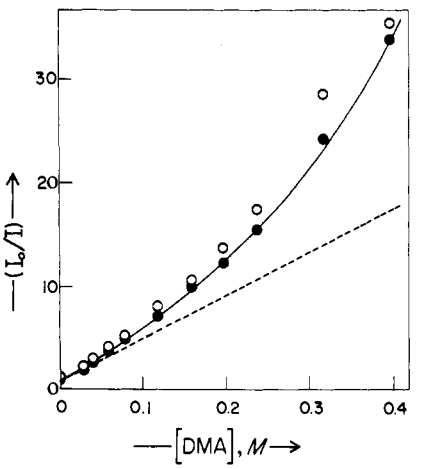

Figure 3. Quenching of steady-state A fluorescence by DMA. The dotted line is from Figure 5.

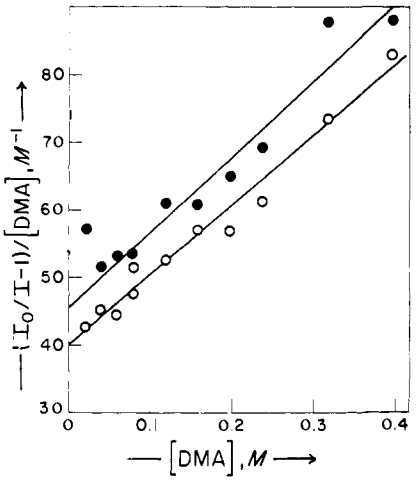

Figure 4. Treatment of A fluorescence data using ground-state (A·DMA) complex model. Full circles in the presence of air.

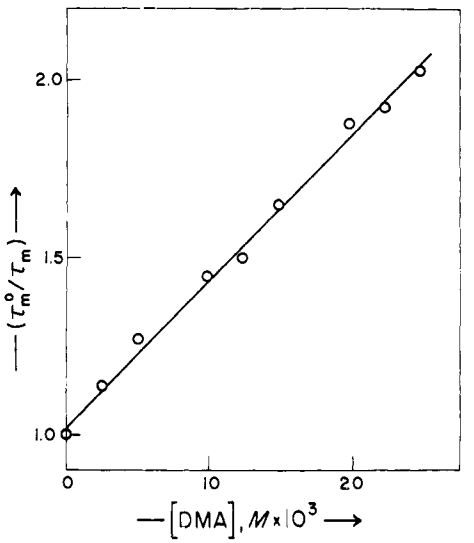

Figure 5. The dependence of ^{1}A* lifetime on [DMA].

$$A + DMA \underset{}{\overset{K_c}{\rightleftharpoons}} (A \cdot DMA) \quad (1)$$

$$A \xrightarrow{h\nu} {}^1A^* \quad (2)$$

$$(A \cdot DMA) \xrightarrow{h\nu} {}^1(A \cdot DMA)^* \quad (3)$$

$${}^1A^* \xrightarrow{k_{fm}} A + h\nu_m \quad (4)$$

$${}^1A^* \xrightarrow{k_{is}} {}^3A^* \quad (5)$$

$${}^1A^* + DMA \underset{k_{-e}}{\overset{k_e}{\rightleftharpoons}} {}^1(A \cdot DMA)^* \quad (6)$$

Assuming that the extinction coefficients of monomer and complex are the same at 352 nm the dependence of I_0/I on [DMA] should be given by

$$I_0/I = \frac{(1 + k_e p \tau_m^0[DMA])(1 + K_c[DMA])}{1 + (1 - p)K_c[DMA]} \quad (7)$$

where $\tau_m^0 = 1/(k_{fm} + k_{is})$ represents the lifetime of ^{1}A* in the absence of DMA, and p represents the fraction of exciplexes which do not regenerate excited monomer. If exciplex formation were irreversible, rearrangement of eq 7, with $p = 1$, to

$$((I_0/I) - 1)/[DMA] = K_c + k_e\tau_m^0 + K_c k_e \tau_m^0[DMA] \quad (8)$$

would allow estimation of K_c and $k_e\tau_m^0$ from a plot of $((I_0/I) - 1)/[DMA]$ vs. [DMA], Figure 4. The line obtained by least-squares analysis gives $K_c = 2.8\ M^{-1}$ and $k_e\tau_m^0 = 37.2\ M^{-1}$. Under the same conditions the dependence of the lifetime of ^{1}A* on [DMA] would be given by

$$\tau_m^0/\tau_m = 1 + k_e\tau_m^0[DMA] \quad (9)$$

The data in Table III plotted in the form of eq 9, Figure 5, give $k_e\tau_m^0 = 40.9\ M^{-1}$ in good agreement with the value obtained from the steady-state fluorescence measurements for $p = 1$. Our experimental value for τ_m^0, 4.42 ± 0.08 ns, differs slightly from the estimate of $\tau_m^0 = 4.25 \pm 0.08$ ns obtained using the small deviation of the intercept in Figure 5 from unity.[36]

The exciplex emission spectra in Figure 1 and the data in Tables I and II show that the exciplex fluorescence quantum yield goes through a maximum value as the concentration of DMA is increased and that an isoemissive point is not maintained for [DMA] > 0.15 M. Other systems for which related spectroscopic observations have been reported are those of naphthalene/1,4-dicyanobenzene,[41] pyrene/*N,N*-dimethylaniline,[42] pyrene/3,5-di-*tert*-butyl-*N,N*-dimethylaniline,[43] and 9,10-dichloroanthracene/2,5-dimethyl-2,4-hexadiene.[33,44] In each of these systems the phenomenon has been attributed to the interception of the exciplex by a second quencher molecule and in two systems[33,41] fluorescence originating from excited heterotrimer species (triplex[33] or exterplex[45]) has been reported. It seems reasonable, therefore, to conclude that the decrease in exciplex emission in the A/DMA system at high [DMA] is explained in the same way

$${}^1(A \cdot DMA)^* + DMA \xrightarrow{k_t} {}^1(A \cdot DMA_2)^* \quad (10)$$

Since no evidence for triplex emission was obtained in this work (with the possible exception of a broadening of the exciplex emission in the lower energy region at the highest DMA concentrations) the postulated formation of a triplex in eq 10 as a distinct species is speculative. Strong support for this hypothesis has been provided recently for the system anthracene/*N,N*-diethylaniline, where triplex formation has been implicated in accounting for the temperature dependence of intersystem crossing yields, fluorescence yields, and fluorescence lifetimes.[46]

If a quenching step involving interaction of the exciplex with DMA, e.g., eq 10, competes with other exciplex decay paths,

$${}^1(A \cdot DMA) \xrightarrow{k_{fe}} (A \cdot DMA) + h\nu_e \quad (11)$$

$${}^1(A \cdot DMA) \xrightarrow{k_{de}} \alpha(A \cdot DMA) + (1 - \alpha)P \quad (12)$$

at low [A], where P represents photoproducts other than dianthracene, then observed exciplex decay rate constants should increase with increasing DMA concentration,

$$k_{obsd} = k_{fe} + k_{de} + k_t[DMA] \quad (13)$$

assuming $p \simeq 1$. The rate constants in Table IV are indeed linearly dependent on [DMA], Figure 6. The slope of the line in Figure 6 gives $k_t = 4.27 \times 10^6\ M^{-1}\ s^{-1}$ and the intercept gives the exciplex decay lifetime $\tau_e^0 = (k_{fe} + k_{de})^{-1} = 120$ ns, where k_{de} represents all first-order exciplex decay paths other than fluorescence. It is now possible to consider whether these k_t and τ_e^0 values are consistent with the experimental exciplex emission quantum yields, ϕ_{fe}, shown in Table II. The mechanism in eq 1-6, and 10-12 predicts that, at low [A], ϕ_{fe} should

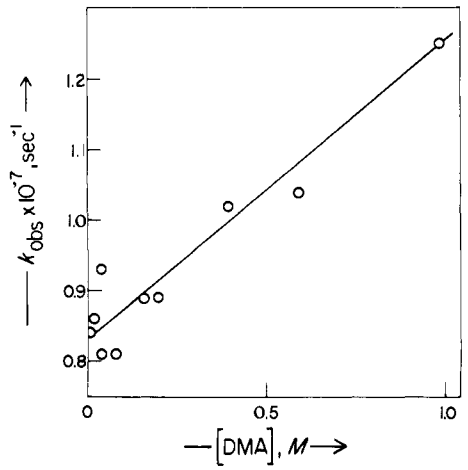

Figure 6. The dependence of ^{1}(A·DMA)* lifetime on [DMA].

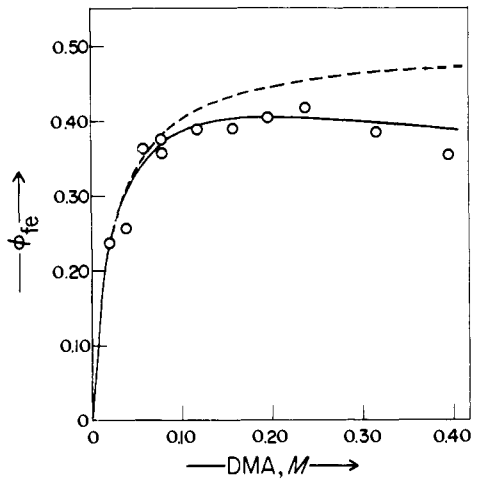

Figure 7. Comparison of calculated (line, eq 15) with experimental (points) ^{1}(A·DMA)* fluorescence quantum yields. The dotted line is for $k_t = 0$.

depend on [DMA] as shown in the equation

$$\phi_{fe} = \left\{\frac{k_e\tau_m^0[DMA] + K_c[DMA](1 + k_e\tau_m^0[DMA])}{(1 + K_c[DMA])(1 + k_e\tau_m^0[DMA])(1 + k_t\tau_e^0[DMA])}\right\} \times k_{fe}\tau_e^0 \quad (14)$$

Since all the constants in eq 14 except k_{fe} have been evaluated, it should be possible to choose a value for k_{fe} which will be consistent with all the ϕ_{fe} values. Alternatively, eq 14 can be shown to be equivalent to

$$\phi_{fe} = (1 - (I/I_0))k_{fe}\tau_e^0/(1 + k_t\tau_e^0[DMA]) \quad (15)$$

where I/I_0 are the experimental A fluorescence intensity ratios. Application of eq 15 to the experimental I_0/I and ϕ_{fe} values in Tables I and II, respectively, for [DMA] $\leq$ 0.4 M using the values of k_t and τ_e^0 obtained from the exciplex decay rate constants gives an average value of $k_{fe}\tau_e^0 = 0.48 \pm 0.02$. This quantity represents the fraction of exciplexes which would fluoresce if second-order decay processes involving interaction with DMA and A were eliminated. It gives $k_{fe} = 4.0_0 \times 10^6$ s^{-1}. At [DMA] = 0.98_6 M the calculated value of $k_{fe}\tau_e^0$ is substantially lower (~0.36), suggesting either that the experimental ϕ_{fe} value is low due to incomplete light absorption by A,[35] or that at high [DMA] the increase in medium polarity causes a decrease in $k_{fe}\tau_e^0$ (cf., however, Figure 6). Comparison of ϕ_{fe} values calculated using eq 15 with experimental ϕ_{fe} values, Figure 7, shows that for [DMA] $\leq$ 0.4 M transient exciplex lifetime measurements are consistent with steady-state fluorescence quantum yield measurements.

The above self-consistent interpretation of the data is based on the assumption that $p \simeq 1$.[47] The presence of the slow decay components in the monomer emission profiles, e.g., Figure 2, of course, shows that p must deviate somewhat from unity.[17] Since the excitation lamp profile and other instrument response functions which distort the decay curves were not determined, the curves could not be analyzed quantitatively. However, an approximate treatment of the data can be carried out as follows. The decay is assumed to be given by a weighted sum of two exponentials,

$$I_m(t) = A_1e^{-\lambda_1 t} + A_2e^{-\lambda_2 t} \quad (16)$$

as in cyclohexane.[17] The slow component parameter λ_2 was assumed equal to 8.4×10^6 s^{-1}, the rate constant of exciplex decay at low [A] and [DMA], Table IV, while the λ_1 was assumed equal to the k_{obsd} values in Table III. The constants A_1 and A_2 were then calculated by fitting eq 16 to the decay profile for t small, $I_m \simeq A_1 + A_2$, and t large, $I_m \simeq A_2e^{-\lambda_2 t}$. An exponential was also empirically fitted to the rise portion of the monomer emission profile. With these constants approximate ratios of the areas corresponding to "prompt" and "delayed" fluorescence were calculated. Quantitative examination of the total emission spectra in Figure 1 shows that a small fraction of the light monitored at 427 nm is due to exciplex emission. The ratio of emission intensities for exciplex and monomer is given by

$$(I_e/I_m)_{427} = 0.026\phi_{fe}/\phi_{fm} \quad (17)$$

This empirical relationship and the ratios of the areas for fast and slow emission allow calculation of prompt and delayed monomer fluorescence quantum yields from the total fluorescence quantum yields in Table II. Two limiting cases were considered in order to estimate equilibrium constants for exciplex formation, K_e. The first assumes fast equilibration of the two excited species relative to decay from either. When this condition holds, following the initial rapid monomer decay, an equilibrium concentration ratio of the two species is maintained and the constant K_e is related to the ratio of exciplex and delayed monomer fluorescence, ϕ_{fm}^d, quantum yields,

$$K_e = (\phi_{fe}/\phi_{fm}^d)(k_{fm}/k_{fe}[DMA]) \quad (18)$$

The second case assumes that exciplex fluorescence from exciplexes formed from ^{1}A* generated by exciplex dissociation is negligible. It then follows that k_{-e}/k_{fe} is given by the quantum yield ratio in the equation

$$k_{-e}/k_{fe} = \phi_{fm}^d/(\phi_{fe}\phi_{fm}^p) \quad (19)$$

K_e can be calculated from this ratio using the value of $k_{fe} = 4.0 \times 10^6$ s^{-1} obtained from the data in Tables II and IV, by assuming that exciplex formation is diffusion controlled, $k_e = k_{dif} = 1.0 \times 10^{10}$ M^{-1} s^{-1}.[48] The fluorescence quantum yields and the K_e values generated for each case are shown in Table X. The condition of rapid reversibility more nearly obtains at high [DMA], while the assumption of no reassociation of ^{1}A* with DMA more nearly obtains at low [DMA]. Apparently, $5 \times 10^3 \leq K_e \leq 9 \times 10^3$ M^{-1} and a value of $K_e \simeq 7 \times 10^3$ M^{-1} at 23–25 °C is probably close to the actual value and may be compared with $K_e = 2.5 \times 10^3$ M^{-1} s^{-1} at 25 °C in cyclohexane.[17] Use of the complete expression in eq 7 and this approximate K_e give $k_e p\tau_m^0 = 38.9$, $K_c = 2.85$ M^{-1}, $p \simeq 0.85$, $k_e \simeq 1.0_3 \times 10^{10}$ M^{-1} s^{-1}, and $k_{-e} \simeq 1.4_7 \times 10^6$ s^{-1}.

Additional information concerning the importance of reversibility in A/DMA exciplex formation is provided by the relative emission intensities obtained from air-saturated solutions, Table I. The intensity ratios at 384 nm are affected very little by the presence of oxygen. The increase at [DMA]

Table X. Apparent K_c Values for Exciplex Formation

[DMA], M × 10^3	$\phi_{fm}{}^p$	$\phi_{fm}{}^d$	$\phi_{fe}{}^a$	K_c, $M^{-1} \times 10^{-3}$ From eq 18[b]	From eq 19[c]
4.93	0.21_4	0.009_5	0.08_4	27	4.7
9.86	0.17_7	0.012_5	0.14_3	18	5.1
14.8	0.14_7	0.017_1	0.18_8	11	4.0
19.7	0.12_6	0.019_5	0.22_1	8.8	3.5
24.7	0.11_2	0.017_4	0.24_9	8.8	4.0

[a] From eq 15, see text. [b] From eq 18, using $k_{fe} = 4.0_3 \times 10^6\ s^{-1}$ and $k_{fm} = 6.1 \times 10^8\ s^{-1}$, see text. [c] From eq 19, see text.

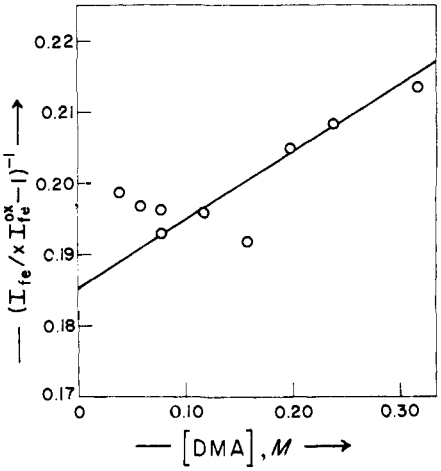

Figure 8. The effect of oxygen on exciplex fluorescence intensity as a function of [DMA], eq 21.

$= 0$ gives $k_{mox}[O_2] = 0.19/\tau_m{}^0 = 4.3 \times 10^7\ s^{-1}$, as expected for diffusion-controlled quenching of $^1A^*$ by oxygen,[33,49]

$$^1A^* + {}^3O_2 \xrightarrow{k_{mox}} {}^3A^* + {}^3O_2 \qquad (20)$$

In the presence of DMA the differences between I_0/I_{ox} and I_0/I ratios are somewhat larger than 0.19, reflecting the small amount of $^1A^*$ formation from the longer lived exciplex, and possibly decreased light absorption by A in the presence of DMA and oxygen. As indicated in the Results, solutions of DMA change from colorless to yellow when oxygen is allowed in the medium, a reversible phenomenon which is almost certainly due to oxygen-enhanced $S_1 \rightarrow T_1$ transitions in a DMA/O_2 complex.[50] In contrast to the small effect of oxygen on monomer emission there is a marked decrease in the intensity of the exciplex emission at 500 nm, last column, Table I. This effect decreases somewhat at the higher DMA concentrations owing, at least in part, to the decreased exciplex lifetime. The exciplex emission ratios in Table I can be treated adequately using eq 21, where x, defined in eq 22, is close to unity ($1.00 \leq x \leq 1.10$) and K_{eox} is the rate constant for the quenching of the exciplex by oxygen, e.g., eq 23.

$$[(I_{deg}/xI_{ox}) - 1]^{-1} = (1 + k_t\tau_e{}^0[DMA])(k_{eox}\tau_e{}^0[O_2])^{-1} \qquad (21)$$

$$x = \left(\frac{k_e\tau_m{}^0[DMA]}{1 + k_e\tau_m{}^0[DMA]} + K_c[DMA]\right) \times \left(\frac{k_e\tau_m{}^0[DMA]}{1 + k_e\tau_m{}^0[DMA] + k_{mox}\tau_m{}^0[O_2] + K_c[DMA]}\right)^{-1} \qquad (22)$$

$$^1(A \cdot DMA)^* + {}^3O_2 \xrightarrow{k_{eox}} {}^3A^* + DMA + {}^3O_2 \qquad (23)$$

This is shown in Figure 8, where the line is drawn using the previously obtained values of k_t and τ_e and $k_{eox}[O_2] = 4.5 \times 10^7\ s^{-1}$, indicating that k_{mox} and k_{eox} are equal within experimental uncertainty. Independent values for $K_{eox}[O_2]$ of 4.2×10^7 and $4.0 \times 10^7\ s^{-1}$ can be based on the observed differences in exciplex lifetime in the presence and in the absence of air, Table V. In the absence of static quenching processes the ratio of monomer fluorescence Stern–Volmer plot slopes for degassed and air-saturated solutions, s and s_{ox}, respectively, is given by the equation[33]

$$s_{ox}/s = (1 + k_{eox}\tau_e{}^0[O_2]) \times \left(\frac{1 + k_{-e}\tau_e{}^0}{1 + k_{-e}\tau_e{}^0 + k_{eox}\tau_e{}^0[O_2]}\right) \qquad (24)$$

Since estimates for all the quantities on the right hand side of eq 24 have been obtained an expected ratio of $s/s_{ox} \simeq 1.14$ can be calculated. This ratio was used to calculate the line drawn for air-saturated solutions in Figure 4. The agreement with the experimental points is satisfactory.

Spectroscopic evidence concerning the possible interaction of the A/DMA exciplex with A is difficult to interpret. Exciplex decay rate constants determined as a function of anthracene concentration in the presence of constant DMA concentrations of 0.0395 and 0.986 M are presented in Table V. Initial measurements were carried out at relatively low [A] ($\leq 4 \times 10^{-3}$ M), since analogy with the anthracene/*trans,trans*-2,4-hexadiene system[2] suggested a very efficient exciplex/anthracene interaction, e.g.,

$$^1(A \cdot DMA)^* + A \xrightarrow{k_t'} {}^1(A_2 \cdot DMA)^* \qquad (25)$$

This [A] range also coincided with the range for which Yang and Shold had previously measured substantial quantum yields for anthracene disappearance, $\phi_{-A} = 0.17 \pm 0.01$ for [DMA] = 1.0 M.[12] Since no change in $^1(A \cdot DMA)^*$ lifetime was noted at these low anthracene concentrations the A concentration range in the presence of 0.986 M DMA was extended to 0.10 M (essentially a saturated A solution in benzene), for which large photodimer yields have been reported.[5,6] A significant increase in the decay rate of the exciplex was now observed, Table V. Neglecting complications which may arise due to reversibility in triplex formation (eq 10 and 25) a linear dependence of k_{obsd} on [A] is expected,

$$k_{obsd} = k_{fe} + k_{de} + k_t[DMA] + k_t'[A] \qquad (26)$$

In view of the relatively large error limits in k_{obsd}, the deviation of the plot in Figure 9 from linearity may not be significant. If the value of 0.090 M A is disregarded, a reasonable straight line can be drawn through the remaining points, which gives $k_t' = 2.0 \times 10^7\ M^{-1}\ s^{-1}$.

Photochemical Observations. Before considering the effect of DMA on anthracene photodimerization, it is appropriate to examine what is known about this reaction in solutions containing no DMA. In a careful study of anthracene dimer yields and anthracene disappearance yields in toluene Suzuki

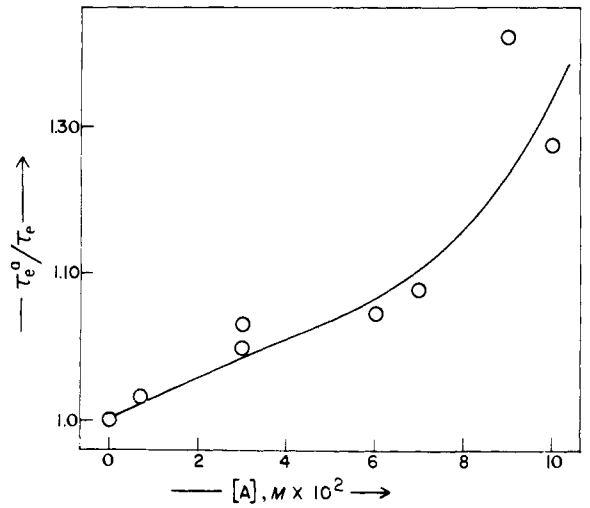

Figure 9. The dependence of ^{1}(A·DMA)* lifetime on [A]; $\tau_e^0 = 81.3$ ns for [DMA] = 0.986 M, Table V.

identified three anthracene concentration egions.[51-53] The relative anthracene dimer yield was found to be independent of anthracene concentration for $7 \times 10^{-3} \leq [A] \leq 1.6 \times 10^{-2}$ M at 30 °C and to increase with anthracene concentration above and below this concentration range. Dimer formation quantum yields were found to increase with temperature (−10 to 30 °C) in this range, up to 0.338 at 30 °C, 366 nm. The range itself appeared to extend to higher anthracene concentrations as the temperature was lowered. The irradiations were apparently carried out in the presence of air, since no deaerating precautions were mentioned and relatively small yields of anthracene peroxide probably account for the small deviations between anthracene losses and dimer yields. Essential features of the photodimerization mechanism suggested in order to account for the peculiar concentration dependence of the quantum yields are summarized in more modern notation[54] in eq 2, 4, 5, 27-30,

$$^1A^* + A \xrightarrow{k_e'} {}^1(AA)^* \quad (27)$$

$$^1(AA)^* \xrightarrow{k_{ed}'} 2A \quad (28)$$

$$^1(AA)^* \xrightarrow{k_{er}'} A_2 \quad (29)$$

$$^1(AA)^* + A \xrightarrow{k_t''} A_2 + A \quad (30)$$

where ^{1}(AA)* represents the excimer.[23] Steps 27-29 show excimer and dimer formation to be sequential processes as suggested by Stevens.[23,53-57] This mechanism predicts the concentration dependence of dimerization quantum yields, ϕ_{A_2}, shown in

$$\phi_{A_2} = \left(\frac{k_e'\tau_m^0[A]}{1 + k_e'\tau_m^0[A]}\right)\left(\frac{k_{er}'\tau_e^{0\prime} + k_t''\tau_e^{0\prime}[A]}{1 + k_t''\tau_e^{0\prime}[A]}\right) \quad (31)$$

where τ_m^0 and $\tau_e^{0\prime}$ are the lifetimes of electronically excited singlet monomer and excimer, respectively, under the conditions of the experiment. Conditions which would yield a concentration-independent region are $k_e'\tau_m^0[A] \gg 1$ and $k_t''\tau_e^{0\prime}[A] \ll 1$, giving $\phi_{A_2} = k_{er}'\tau_e^{0\prime}$. Since the plateau is reached at $[A] \simeq 7 \times 10^{-3}$ M and $\tau_m^0 \simeq 4 \times 10^{-9}$ s (4.4 ns for degassed benzene solutions and 3.7 ns in the presence of air) the first condition requires $k_e' \gg 3 \times 10^{10}$ M^{-1} s^{-1}, a much larger value than the limit of 1.0×10^{10} M^{-1} s^{-1} for a diffusion-controlled process. It is clear, therefore, that the simple mechanism suggested by Suzuki, eq 27-30, does not account for his observations. Suzuki's plateau is absent from Bowen

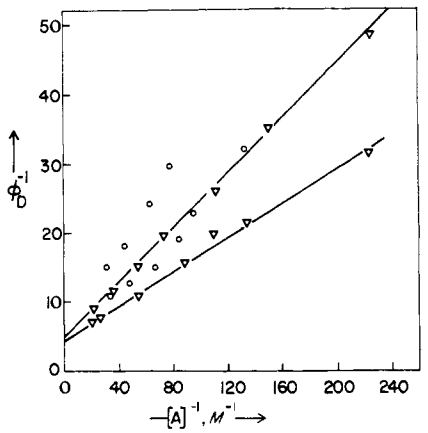

Figure 10. The dependence of $\phi_{A_2}^{-1}$ on $[\bar{A}]^{-1}$; ▽, this work, lower points degassed solutions, upper points air saturated; ○, from ref 56, lower points air saturated; upper points oxygen saturated.

and Tanner's observations in benzene.[58] These workers vigorously rolled the samples during the irradiations, which were carried out in the presence of air or pure oxygen. Anthracene photooxidation quantum yields were also determined.[58] The photodimerization mechanism must now include oxygen's quenching of ^{1}A*, eq 20, and possibly the quenching of excimers by oxygen,[2]

$$^1(AA)^* + O_2 \xrightarrow{k_{eox}'} 2A + O_2 \quad (32)$$

In the presence of oxygen any contribution of anthracene triplets to the photodimerization can be neglected.[59] A linear dependence of $\phi_{A_2}^{-1}$ on $[A]^{-1}$ is predicted if it is assumed that Suzuki's trimeric process, eq 30, is not operative,

$$\phi_{A_2}^{-1} = \left(1 + \frac{1 + k_{mox}\tau_m^0[O_2]}{k_e'\tau_m^0[A]}\right) \times \left(\frac{1 + k_{eox}'\tau_e^{0\prime}[O_2]}{k_{erbase'}\tau_e^{0\prime}}\right) \quad (33)$$

The adherence of Bowen and Tanner's data to eq 33 is adequate and the data are consistent with $k_e'\tau_m^0 = 30$ M^{-1} obtained for the self-quenching of anthracene fluorescence in benzene[62] at "ordinary temperature", ≃15 °C.[63] The data are not sufficiently precise to evaluate the importance of eq 32 and thus do not address the question of an excimer intermediate in the photodimerization.

Excimer fluorescence has been observed in glassy[64] and crystalline media,[65] and recently a weak fluorescence has been assigned to the excimer in a concentrated anthracene solution in toluene.[66] Excimer lifetimes as high as 8 ns and as low as ≤1.5 ns have been inferred from oxygen quenching,[2] and excitation transfer[67] experiments, respectively.

Initial anthracene disappearance quantum yield measurements in this work were irreproducible and behavior similar to that reported by Suzuki was observed for solutions which were open to air. Results in agreement with eq 33 were obtained when little magnets were included in each sample tube and solutions were magnetically stirred throughout the irradiation period. Anthracene disappearance quantum yields calculated from the results in Table VI are shown in Table XI. The quantum yields for air-saturated solutions are in close agreement with those of Bowen and Tanner, and are converted to photodimerization quantum yields by subtracting the photooxidation yields observed by these workers, $\phi_{A_2} = \frac{1}{2}(\phi_{-A} - \phi_{AO_2})$.[58,68] Plots of $\phi_{A_2}^{-1}$ vs. the inverse of the average anthracene concentration, $[\bar{A}]^{-1}$, are linear, Figure 10, as required by eq 33 and confirm the conclusion that the interaction of excimer with anthracene, eq 30, is not an important dimer forming step. The intercept to slope ratios for the degassed and

Table XI. Anthracene Disappearance and Dimerization Quantum Yields

Degassed			Air		
$[A]_0$, $M \times 10^2$	ϕ_{-A}	ϕ_{A_2}	$[A]_0$, $M \times 10^2$	ϕ_{-A}	ϕ_{A_2}[a]
0.50_5	0.064_1	0.032	0.50_0	0.049_0	0.021
0.83_3	0.094	0.047	0.75	0.071_5	0.030
1.01	0.101	0.050	1.00	0.090_5	0.038
1.25	0.129	0.065	1.50	0.122	0.051
2.02	0.190	0.095	2.00	0.156	0.065
4.17	0.254	0.127	3.00	0.208	0.086
5.05	0.289	0.145	5.00	0.268	0.110

[a] Corrected for peroxidation using $\phi_{AO_2}^{-1} = 8.5_6 + (0.548/[A])$ from ref 58.

air-saturated lines are 37.8 and 25.7 M^{-1}, respectively. The mechanism requires that the ratio of these values, 1.47, equal $(1 + K_{mox}\tau_m^0[O_2])$, which has been determined spectroscopically to be 1.19, Table I. The deviation between these two values may be due in part to small differences between the photooxidation quantum yields determined by Bowen and Tanner and those applicable to our conditions. The value of $k_e'\tau_m^0 = 37.8\ M^{-1}$ at $\simeq 23$ °C is in good agreement with Bowen's value of 30 M^{-1} obtained from the self-quenching of anthracene fluorescence at $\simeq 15$ °C.[62,63] The ratio of T/η for these two temperatures is 1.16,[69] suggesting that $k_e'\tau_m^0 = 35\ M^{-1}$ would be exactly consistent with Bowen's result.[68] The possibility of a triplet path to dimerization involving self-quenching in degassed solutions is therefore ruled out. Our value and the anthracene singlet lifetime give $K_e' = 8.5 \times 10^9\ M^{-1}\ s^{-1}$, indicating that excimer formation is an essentially irreversible diffusion-controlled process (i.e., $p \geq 0.8$). The intercepts of the lines in Figure 10 are 4.57 and 4.93 for the degassed and air-saturated data, respectively. The first gives $k_{er}'\tau_e^{0\prime} = 0.22$ as the limiting quantum yield for anthracene dimerization at infinite anthracene concentration, in good agreement with the value of 0.24 reported recently for toluene solutions,[66] and represents the fraction of excimers which give dimer. In this connection it is interesting to note that the quantum yield of A_2 cleavage in degassed cyclohexane solution has been found to be 0.70.[70] Since, barring an unforeseen solvent effect, the sum of the cleavage quantum yield and the limiting dimerization quantum yield, 0.92, is nearly unity, it is likely that the excimer is a common intermediate for the two reactions. The difference in the intercepts in Figure 10 gives $k_{eox}'\tau_e^0[O_2] = 0.08$ as a rather imprecisely determined quantity. Using $k_{eox}'[O_2] = k_{mox}[O_2] = k_{eox}[O_2] \simeq 4 \times 10^7\ s^{-1}$ gives an excimer lifetime $\tau_e^{0\prime} = 2$ ns.[71] Experiments using pure oxygen over the samples together with precise determination of photooxidation yields should provide a more difinitive characterization of the excimer.[71]

Our results provide a tentative explanation for the anomalous concentration dependence observed by Suzuki.[51-53] When a scaling factor is used on Suzuki's relative quantum yields (his absolute quantum yields are much larger than our own) the low anthracene concentration data fall close to our values for air-saturated solutions, while at high anthracene concentrations Suzuki's data correspond closely to values for our degassed solutions. Apparently, oxygen depletion and concentration gradients in the unstirred solutions are responsible for this behavior.

It is now possible to consider the photochemical observations in the presence of DMA. The data in Table VII are converted to quantum yields in Table XII. In the absence of air the anthracene loss should be accounted for by formation of dimer and of products arising from interaction with DMA, i.e., $\phi_{-A} = 2\phi_{A_2} + \phi_P$. Approximate values of ϕ_{A_2} and ϕ_P can be obtained by plotting the percent dimer yield vs. the average anthracene concentration, Table IX, and estimating by interpolation the fraction of anthracene loss due to dimer formation for each concentration in Table XII. The ϕ_{A_2} and ϕ_P values obtained in this way are shown in Table XII.

Table XII. Anthracene Disappearance Quantum Yields in the Presence of DMA

$[A]_0$, $M \times 10^2$	[DMA], $M \times 10^2$	ϕ_{-A}	ϕ_{A_2}[a]	ϕ_P[a]
0.72_6	3.9_4	0.059	0.018	0.022
1.33	3.9_4	0.072_4	0.027	0.019
2.53	3.9_4	0.13_3	0.059	0.015
3.61	3.9_4	0.20_5	0.097	0.012
4.75	3.9_4	0.21_5	0.104	0.006_5
4.81	3.9_4	0.22_2	0.108	0.006
6.03	3.9_4	0.251	0.123	0.005
7.50	3.9_4	0.281	0.136	0.008
0.30_0	$98._4$	0.19_1	0.001_4	0.18_8
0.60_1	$98._4$	0.19_1	0.002_7	0.18_6
1.2_0	98.4	0.19_2	0.005_7	0.18_2
2.4_0	98.4	0.19_7	0.012_1	0.17_3
3.0_3	98.4	0.23_3	0.019_3	0.19_4
3.6_1	98.4	0.23_7	0.024_4	0.18_8
4.0_0	98.4	0.25_1	0.028_4	0.19_4
4.8_1	$98._4$	0.25_2	0.036_9	0.17_8
5.9_9	98.4	0.23_7	0.045	0.14_7
8.2_6	$98._4$	0.25_5	0.075	0.104

[a] See text.

The mechanism of anthracene dimer formation in the presence of DMA is complex. For the sake of clarity this discussion begins with the simplest case and new steps are added to the mechanism as needed. Assuming first that dimer arises only from the excimer and that exciplex formation is a competitive process which quenches dimerization, the dimerization quantum yield is given by

$$\phi_{A_2} = \left(\frac{1 + (1 - p')K_c[DMA]}{K_c[DMA] + 1}\right) k_{er}'\tau_e^{0\prime} \times \left(\frac{k_e'\tau_m^0[A]}{1 + k_e'\tau_m^0[A] + k_e p'\tau_m^0[DMA]}\right) \quad (34)$$

where $p' = (1 + k_t\tau_e^0[DMA] + k_t'\tau_e^0[A])/(1 + k_{-e}\tau_e^0 + k_t\tau_e^0\ [DMA] + k_t'\tau_e^0[A])$. We consider first the high DMA concentration data for which, according to the spectroscopic observations, most $^1A^*$ are either born associated with or become quickly bound to one or more DMA molecules. Except for p', which must be close to unity, all the parameters in eq 34 have been determined. Using $k_{-e}\tau_e^0 = 0.176$, $k_t\tau_e^0 = 0.512\ M^{-1}$, and $k_t'\tau_e^0 = 2.4\ M^{-1}$ it can be shown that, for [DMA] = 0.984 M, $p' = 0.90$ at low [A] and approaches 0.91 as [A] is increased to the saturation limit. For example, for [A] = 0.06 and [DMA] = 0.984 M eq 34 gives $\phi_{A_2} = 0.0038$, which is a full order of magnitude smaller than the experimental quantum

yield, Table XII. This is compelling evidence for a dimer forming pathway via the exciplex. An attractive possibility is formation of an $^1(A_2 \cdot DMA)^*$ triplex, eq 25, followed by its decay,

$$^1(A_2 \cdot DMA)^* \xrightarrow{k_{td}'} \beta A_2 + DMA + (1 - \beta)(2A + DMA) \quad (35)$$

where β is the fraction of $^1(A_2 \cdot DMA)^*$ triplexes which give dimer. Dimer could form directly or following dissociation of the triplex to the excimer. Alternatively, the interaction of anthracene with the exciplex could be a substitution process leading smoothly to excimer formation.[72] An additional pathway for dimer formation is provided by the interaction of excimers with DMA, e.g., the equation[3]

$$^1(AA)^* + DMA \xrightarrow{k_t'''} {}^1(A_2 \cdot DMA)^* \quad (36)$$

This mechanism has been suggested to be important for substituted anthracenes and could give dimer directly without a triplex intermediate.[3] Inclusion of eq 35 and 36 in the mechanism gives

$$\phi_{A_2} = \left(\frac{1}{K_c[DMA] + 1}\right)\left[\left(1 + (1 - p')K_c[DMA]\right) \times \left(\frac{k_{er}'\tau_e^{0\prime} + \beta k_t'''\tau_e^{0\prime}[DMA]}{1 + k_t'''\tau_e^{0\prime}[DMA]}\right) \times \left(\frac{k_e'\tau_m^0[A]}{1 + k_e'\tau_m^0[A] + k_e p'\tau_m^0[DMA]}\right) + \left(\frac{\beta k_t'\tau_e^0[A]}{1 + k_{-e}\tau_e^0 + k_t\tau_e^0[DMA] + k_t'\tau_e^0[A]}\right) \times \left(K_c[DMA] + \frac{k_e\tau_m^0[DMA]}{1 + k_e'\tau_m^0[A] + k_e p'\tau_m^0[DMA]} \times (1 + (1 - p')K_c[DMA])\right)\right] \quad (37)$$

which replaces eq 34 in describing the dependence of the dimer quantum yield on [A] and [DMA]. The first product of terms in eq 37 corresponds to the excimer pathway for dimer formation, and the second product of terms gives the contribution of the exciplex to dimer formation. It can easily be seen that the excimer pathway should dominate for [DMA] = 0.0394 M, while the exciplex pathway should dominate for [DMA] = 0.984 M. If the mechanism considered thus far were complete it would be possible to predict the ϕ_{A_2} values in Table XII by choosing appropriate values for β and $k_t'''\tau_e^{0\prime}$, the two remaining unknown parameters in eq 37. Although it was not possible to fit the data quantitatively with eq 37, certain conclusions seem warranted. The experimental dimerization quantum yields at [DMA] = 0.0394 M adhere closely to values predicted by eq 34.[73] Since eq 34 is equivalent to the first product of terms in eq 37, with $k_t'''\tau_e^{0\prime} = 0$, it follows that the enhanced dimerization pathway via the interaction of the excimer with DMA is probably not important in this system. An attempt was made to fit the ϕ_{A_2} values for [DMA] = 0.984 M with eq 37. Using $k_t' = 2.0 \times 10^7\ M^{-1}\ s^{-1}$ an excellent fit is obtained for $2.29 \times 10^{-2}\ M \leq [A]$ with $\beta = 0.30$, but at higher anthracene concentrations larger values of β are required, Table XIII. This behavior suggests that the nonlinearity in Figure 9 is real and that the mechanism considered thus far is not complete. It is possible, for example, that reversibility in trriplex formation, eq 10 and 25, gives rise to some coupling of the exciplex lifetime with those of the triplexes.[46,47] A further possibility is that at high anthracene concentrations part of the emission monitored at 500 nm comes from the $^1(A_2 \cdot DMA)^*$ triplex, so that the changes attributed t τ_e may be due in part to changes in τ_t'. It seems premature to consider possible isomeric donor–acceptor sequences in the triplexes, but it is obvious that if in $^1(A \cdot DMA_2)^*$ the anthracene is sandwiched between two DMA molecules, this triplex would have to dissociate before any A_2 could form. Similarly, if the DMA in $^1(A_2 \cdot DMA)^*$ were sandwiched between two anthracene molecules, it would not be a likely direct source of A_2. Scheme I summarizes the processes which appear to be important in determining the spectroscopy and chemistry of this system. The rate constants evaluated in this work are summarized in Table XIV.

Table XIII. Effective β Values

$[\bar{A}]$, $M \times 10^2$	$\phi_{A_2}^{c\prime}$, $\times 10^3$	$\phi_{A_2}^{c}/\beta$, $\times 10^3$	β^a
0.25	0.17	3.93	0.31
0.55	0.37	8.61	0.27
1.10	0.74	17.0	0.29
2.29	1.51	34.7	0.30
2.93	1.92	43.9	0.39
3.42	2.23	50.8	0.44
4.60	2.95	66.9	0.51
5.74	3.63	81.8	0.51
8.00	4.9	110.0	0.64

[a] Calculated from $(\phi_{A_2}^{obsd} - \phi_{A_2}^{c\prime})\beta/\phi_{A_2}^{c}$ where $\phi_{A_2}^{obsd}$ is the observed quantum yield and $\phi_{A_2}^{c\prime}$, $\phi_{A_2}^{c}$ are the calculated excimer and exciplex dimerization components, eq 37.

Scheme I. Summary of A/DMA Interactions

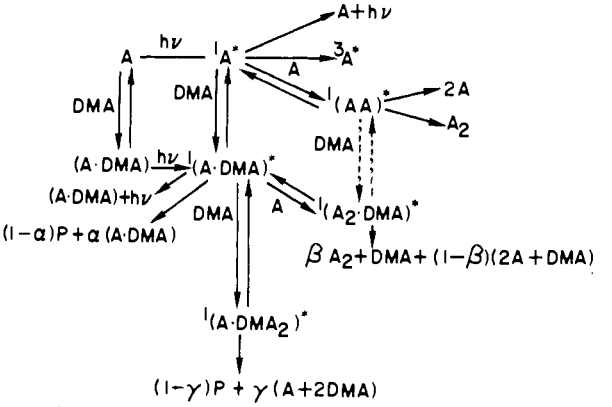

The study of products other than dianthracene was not pursued, since such a study was undertaKen by Professor N. C. Yang.[74] Consideration of the approximate ϕ_P values in Table XII tends to support the major mechanistic conclusion that a second DMA molecule plays an important part in product formation, e.g., eq 10, followed by[74]

$$^1(A \cdot DMA_2)^* \xrightarrow{k_{td}} (1 - \gamma)P + \gamma(A + 2DMA) \quad (38)$$

Briefly, since at 0.039 M DMA and low [A] ~64% of $^1A^*$ emission is quenched, Table I, and ϕ_{A_2} is negligible, if the exciplex were the sole precursor to the other products, then $\phi_{-A} \simeq \phi_P \simeq 0.64(1 - \alpha)$. If, furthermore, the interaction of the exciplex with DMA produced no products, ϕ_P, which could at best attain the limiting value of $(1 - \alpha)$, should decrease drastically at 1 M DMA. The opposite is observed. Inclusion of eq 38 in the mechanism gives

$$\phi_P = \frac{(1 - \alpha) + (1 - \gamma)k_t\tau_e^0[DMA]}{(1 + K_{-e}\tau_e^0 + k_t\tau_e^0[DMA] + k_t'\tau_e^0[A])(K_c[DMA] + 1)} \times \left[K_c[DMA] + \frac{k_e\tau_m^0[DMA](1 + [1 - p']K_c[DMA])}{1 + k_e'\tau_m^0[A] + k_e p'\tau_m^0[DMA]}\right] \quad (39)$$

Table XIV. Summary of Rate Constants[a]

Process	Symbols	Value
Unimolecular decay of $^1A^*$	$(k_{fm} + k_{is})$, $1/\tau_{fm}^0$	$2.2_6 \times 10^8$ s^{-1}
Formation of $^1(A{\cdot}DMA)^*$	k_e	$1.0_3 \times 10^{10}$ M^{-1} s^{-1}
Dissociation of $^1(A{\cdot}DMA)^*$	k_{-e}	1.5×10^6 s^{-1}
Unimolecular decay of $^1(A{\cdot}DMA)^*$	$k_{fe} + k_{de}$, $1/\tau_e^0$	8.3×10^6 s^{-1}
Fluorescence of $^1(A{\cdot}DMA)^*$	k_{fe}	4.0×10^6 s^{-1}
Nonradiative decay of $^1(A{\cdot}DMA)^*$	$k_{de} + k_{-e}$	4.3×10^6 s^{-1}
P formation from $^1(A{\cdot}DMA)^*$	$(1 - \alpha)k_{de}$	2.1×10^5 s^{-1}
Formation of $^1(A{\cdot}DMA_2)^*$ from $^1(A{\cdot}DMA)^*$	k_t	$4.2_7 \times 10^6$ M^{-1} s^{-1}
Formation of $^1(A_2{\cdot}DMA)^*$ from $^1(A{\cdot}DMA)^*$	k_t'	$\sim 2.0 \times 10^7$ M^{-1} s^{-1}
Quenching of $^1A^*$ by O_2	$k_{mox}[O_2]$	4.3×10^7 s^{-1}
Quenching of $^1(A{\cdot}DMA)^*$ by O_2	$k_{eox}[O_2]$	$(4.0\text{–}4.5) \times 10^7$ s^{-1}
Formation of excimer	k_e'	8.5×10^9 M^{-1} s^{-1}
Unimolecular decay of excimer	$k_{ed}' + k_{er}'$, $1/\tau_e^{0\prime}$	$(5\text{–}1.7)^b \times 10^8$ s^{-1}
Fraction of $^1(AA)^*$ giving A_2	$k_{er}'\tau_e^{0\prime}$	0.22
Fraction of $^1(A{\cdot}DMA_2)^*$ giving P	$(1 - \gamma)$	0.54

[a] All values for benzene solutions at 23–25 °C. [b] See text and footnote 71.

for the dependence of ϕ_P on [A] and [DMA]. Once again, reversibility in triplex and excimer formation was neglected. Using eq 39 and ϕ_P values of 0.022 and 0.18 for DMA concentrations of 0.039 and 0.984, respectively, and low [A] gives $(1 - \alpha) = 0.016$ and $(1 - \gamma) = 0.54$ for the efficiencies of product formation from exciplex and triplex, respectively. These product efficiencies refer only to reactions other than dianthracene formation which consume anthracene, and it is not known whether the same or different product distributions are obtained from exciplex and triplex. The character of these products could also change due to concentration dependent behavior of subsequently formed intermediates, e.g., triplet states[46] or ion radicals.

The dimer yields obtained in this work are considerably lower than those reported earlier.[5,6] Examination of the observations in Table IX does show that higher dimer yields are achieved when air is present during the irradiation. Also, the yields decrease when the reactions are allowed to proceed until all the anthracene is destroyed, consistent with the expected increase in ϕ_P/ϕ_{A_2} as [A] is decreased. The effect of air on ϕ_P was measured, Table VIII, in order to determine whether the quenching of the nondimer products parallels the quenching of the exciplex by oxygen. It was reasoned that oxygen might have a more significant effect on ϕ_P if it also intercepted longer lived intermediates such as ion radicals, whose formation in the A/DMA system in acetonitrile has been confirmed by flash spectroscopy.[28] For example, interaction of anthracene anion radicals with oxygen could give anthracene and result in enhanced dianthracene yields. The observed $\phi_P/\phi_P^{O_2}$ ratios of 3.5–3.9 in 0.986 M dimethylaniline are, however, even smaller than those expected for the quenching of the exciplex, ~4.5 (extrapolated from Table I). Use of a Pyrex filter instead of a 366-nm filter also increased dimer yields, Table IX. It is possible that prolonged irradiation with higher frequency light in the presence of air leads to regeneration of anthracene from other products. The possibility that the other products sensitize the formation of dianthracene is ruled out by the data in Table IX (compare rows 9 and 10).

Experimental Section

Materials. Most spectroscopic measurements were made using anthracene (Eastman, blue-violet fluorescence), which was chromatographed on alumina with benzene as eluent, mp 215.6–216.1 °C. Photochemical measurements were carried out using anthracene (Matheson, Coleman, and Bell, blue-violet fluorescence) without purification. In one set of experiments anthracene synthesized from dianthracene was also used. The dianthracene, 0.9 g, prepared by irradiation of a degassed benzene solution of anthracene was recrystallized from 450 ml of toluene (Mallinckrodt, analytical reagent). Approximately half of the sample dissolved and 0.41 g of white crystals was obtained upon cooling the filtered solution. This material was charged into a 10-cm piece of 5-mm glass tubing, which was then sealed at both ends at atmospheric pressure. The tubing was floated in a Wood's metal bath at ~250 °C for 40 min, until all the crystals had turned to a yellow melt. The anthracene was chromatographed on alumina with methylene chloride as eluent, and the light yellow product was sublimed under vacuum to give 0.37 g of white crystals. This material had identical UV absorption characteristics and gave identical photochemical results as the unpurified anthracene.

N,N-Dimethylaniline, Aldrich reagent, was purified by distillation over mossy zinc under reduced pressure, bp 90.0–90.5 °C, immediately before use. Benzene, spectral grade from Mallinckrodt, Baker, or Fisher, was used for spectroscopic measurements without purification. Most quantum yield measurements were carried out using benzene purified by the Metts procedure by exhaustive photochlorination of hydrocarbon impurities.[75] No difference could be detected in results using purified or unpurified benzene. *trans*-Stilbene, Aldrich zone-refined, was used without purification. It contained 0.04% cis isomer, GLC. *cis*-1,3-Pentadiene, Columbia Organic Chemicals, was bulb-to-bulb distilled immediately prior to use. It contained 0.3% trans isomer, GLC. Benzophenone, Aldrich reagent, was recrystallized from *n*-pentane three times and sublimed, mp 47.5–48.5 °C.

Fluorescence Measurements. Steady-state fluorescence measurements were made using a Perkin-Elmer Hitachi MPF-2A spectrophotometer as previously described.[33]

Fluorescence Lifetimes. Procedure 1 was that described in ref 33, and was used to monitor anthracene monomer emission. Procedures 2 and 3 were used to monitor the exciplex emission at 500 nm. In procedure 2 fluorescence was determined by analogue detection. Samples were placed in 5 mm × 8 cm Pyrex tubes and degassed with five to six freeze–pump–thaw cycles down to 10^{-5}–10^{-6} Torr. The sample cells were side-pumped with 337-nm irradiation from an AVCO-Everett C950 nitrogen laser operating at 40 Hz. The fluorescence, monitored from the end of the sample cell, was filtered with a Corning 3-72 filter and focused on the entrance slit of a Jarrell-Ash ¼ M monochromator. An RCA 8850 photomultiplier was mounted on the exit slit of the monochromator. The fluorescence decay was observed directly by routing the output of the photomultiplier, which was operated at −1400 V through a 50-Ω load resistor to a Tektronix 454 oscilloscope. Photographs were taken of the oscilloscope display of the fluorescence decay. The photographs were enlarged by projection and values of the fluorescence intensity as a function of time were measured with a ruler. Lifetimes were determined from the slopes of first-order plots which exhibited excellent linearity. Procedure 3 also employed analogue detection. In this case samples were enclosed in 4-mm o.d. by 3 in. long Pyrex tubes. One end of the tube was shaped to form a hemispherical lens, while at the other end a sidearm was attached which allowed convenient degassing of the sample (as in procedure 2) before transfer to the 3-in. tube. The AVCO-Everett C950 nitrogen laser operated at 50 pps and at voltages ranging from 13 to 15 kV was used to side-pump the sample tubes. Strong green emission was observed at the hemispherical lens, since fluorescence is partially collected along the length of the tube by total internal re-

flection. Fluorescence decay profiles were monitored with a IP 21 tube operated at 400–500 V. Since the nitrogen laser light was filtered with a 334-nm line filter (Ealing) and emission was observed through a 566-nm interference filter (Optics Technology) and a Corning 3-67 filter, scattered excitation light was not monitored by the phototube. A PAR Model 115 preamplifier with gain of 10 was used to impedance match the tube anode to a Tektronix 453A oscilloscope with camera attachment. Exposures (1 s) at $f/4$ were sufficient to obtain well-defined decay curves. Maximum amplitudes were about 300 mV. All lifetime measurements were made at 25 ± 1 °C.

Absorption Measurements. Ultraviolet absorption spectra were obtained using a Cary 14 recording spectrophotometer. Infrared absorption spectra of Nujol mulls were recorded using Perkin-Elmer Model 137 and Model 521 spectrophotometers.

Irradiation Procedures. Two procedures were employed for quantum yield measurements. In procedure 1 a Moses merry-go-round apparatus[76] immersed in a thermostated water bath and a 200-W Hanovia medium pressure mercury lamp in a Pyrex cooling probe were employed. The 366-nm mercury lines were isolated using Corning CS 7-37 and 0-52 filters. In procedure 2 sample tubes (up to eight) were irradiated in a small cylindrical merry-go-round attached to a stirring motor, Gerald K. Heller Co., Model G.T.21, which allowed rotation of the samples over a magnetic stirrer. Light from an Osram HBO 200-W super-pressure mercury lamp in a Bausch and Lomb housing was collimated, then made to converge on the sample tubes using appropriate lenses. Corning filters CS 7-37 and 0-52 were placed between the lenses to isolate the 366-nm mercury lines. For both procedures samples (2.6–3.0 ml) of solutions containing the desired substrates were introduced into 13 × 60 mm Pyrex ampules equipped with grease traps and 10/30 ☤ female joints. Solutions were degassed using four to five freeze–pump–thaw cycles to 10^{-5}–10^{-6} Torr and ampules were flame sealed at a constriction. In many instances extra tubes were degassed and were used as reference in the UV measurements. In procedure 2 tiny magnets were included in each tube for individual stirring of the irradiated solutions. Anthracene alone solutions irradiated in the presence of air were equipped with 10/30 ☤ stoppers. The irradiation was stopped periodically and 5-ml air samples were bubbled by syringe through the solutions. The irradiations were carried out at room temperature and the temperature monitored periodically close to the samples (23.0 ± 1.0 °C). Stilbene and 1,3-pentadiene solutions were analyzed by GLC as previously described,[19,77] except that Varian-Aerograph instruments 940 and 2700 were employed.

For dianthracene gravimetric determinations at 25 °C, 75- or 80-ml aliquots of the desired solution were syringed into 18 cm × 5 cm o.d. Pyrex ampules equipped with 14/35 ☤ female joints and grease traps. The solutions were degassed using four freeze–pump–thaw cycles and flame sealed at a constriction. Irradiations were performed using a 450-W medium-pressure mercury Hanovia lamp in a Pyrex water-cooled probe. Corning filters CS 7-37 and 0-52 were used to isolate the 366-nm mercury lines. The ampule and probe were immersed in a thermostated water bath. Following irradiation an aliquot was used for UV analysis and the remaining solution was concentrated, precipitated dimer was washed with cold benzene, dried, and weighed. The solubility of dianthracene in benzene was found to be 0.19 mg/ml; however, the rate of solution was extremely slow and heating was necessary. In the case of the most dilute anthracene solution, 1.0×10^{-3} M, the irradiation of 800 ml of solution was carried out in 265-ml portions in a Hanovia reactor using a 200-W medium-pressure mercury Hanovia lamp in a Pyrex probe equipped with a cylindrical uranium glass filter. Nitrogen was bubbled through the solution 1 h before and throughout each irradiation. The solvent was removed with a rotoevaporator. The white solid was extracted with 25 ml of benzene to dissolve unreacted A. The precipitate was washed with cold benzene, dried, and weighed. For irradiations through Pyrex the 450-W lamp was used and samples containing 3–5-ml aliquots were placed in a thermostated bath, 30 °C. No attempt was made in these experiments to isolate dimer dissolved in the solvent. In all cases the identity of the precipitates as pure dianthracene was established by IR.

References and Notes

(1) (a) Supported by National Science Foundation Grants No. MPS 74-21093 and MPS 76-02439 and by a contract between the Division of Biomedical and Environmental Research, U.S. Atomic Energy Commission, and Florida State University. (b) Presented in part at the meeting of the Florida Section of the American Chemical Society, March, 1974, Tallahassee, Florida, Abstract No. 37. (c) Department of Chemistry. (d) Institute of Molecular Biophysics.

(2) J. Saltiel and D. E. Townsend, *J. Am. Chem. Soc.*, **95**, 6140 (1973).

(3) Cf., also, R. O. Campbell and R. S. H. Liu, *Chem. Commun.*, 1191 (1970); *Mol. Photochem.*, **6**, 207 (1974).

(4) A weak emission which appears to originate from the anthracene/2,4-hexadiene exciplex has been observed: B. D. Watson, D. E. Townsend, and J. Saltiel, *Chem. Phys. Lett.*, **43**, 295 (1976).

(5) C. Pac and H. Sakurai, *Tetrahedron Lett.*, 3829 (1969).

(6) R. S. Davidson, *Chem. Commun.*, 1450 (1969).

(7) N. Mataga and T. Kubota, "Molecular Interactions and Electronic Spectra", M6rcel DekKer, New York, N.Y., 1970, p 442.

(8) H. Beens, H. Knibbe, and A. Weller, *J. Chem. Phys.*, **47**, 1183 (1967).

(9) H. Knibbe, K. Rollig, F. P. Schafer, and A. Weller, *J. Chem. Phys.*, **47**, 1184 (1967).

(10) A. Weller in "Fast Reactions and Primary Processes in Chemical Kinetics", S. Claesson, Ed., Wiley-Interscience, New York, N.Y., 1967.

(11) We are grateful to Professor N. C. Yang for informing us of related observations in his laboratory.[12]

(12) N. C. Yang and D. M. Shold, unpublished observations.

(13) W. R. Dawson and M. W. Windsor, *J. Phys. Chem.*, **72**, 3251 (1968).

(14) J. B. Birks and D. J. Dyson, *Proc. R. Soc. London, Ser. A.*, **275**, 135 (1963).

(15) G. Weber and F. W. J. Teale, *Trans. Faraday Soc.*, **53**, 646 (1957).

(16) W. H. Melhuish, *J. Phys. Chem.*, **65**, 229 (1961).

(17) M.-H. Hui and W. R. Ware, *J. Am. Chem. Soc.*, **98**, 4718 (1976). We thank Professor W. R. Ware for a preprint of this paper.

(18) A. A. Lamola and G. S. Hammond, *J. Chem. Phys.*, **43**, 2129 (1965).

(19) J. Saltiel, D. E. Townsend, and A. Sykes, *J. Am. Chem. Soc.*, **95**, 5968 (1973).

(20) H. A. Hammond, D. E. DeMeyer, and J. L. R. Williams, *J. Am. Chem. Soc.*, **91**, 5180 (1969).

(21) D. Valentine, Jr. and G. S. Hammond, *J. Am. Chem. Soc.*, **94**, 3449 (1972).

(22) V. R. Rao and V. Ramakrishnan, *Chem. Commun.*, 971 (1971).

(23) For a review see B. Stevens, *Adv. Photochem.*, **8**, 161 (1971).

(24) N. C. Yang and J. Libman, *J. Am. Chem. Soc.*, **95**, 5783 (1973).

(25) H. Leonhardt and A. Weller, *Ber. Bunsenges. Phys. Chem.*, **67**, 791 (1963).

(26) H. Knibbe, D. Rehm, and A. Weller, *Ber. Bunsenges. Phys. Chem.*, **72**, 257 (1968).

(27) Y. Taniguchi, Y. Nishima, and N. Mataga, *Bull. Chem. Soc. Jpn.*, **25**, 764 (1972).

(28) Y. Taniguchi and N. Mataga, *Chem. Phys. Lett.*, **13**, 596 (1972).

(29) For a review see M. Ottolenghi, *Acc. Chem. Res.*, **6**, 153 (1973).

(30) F. Perrin, *C. R. Acad. Sci.*, **178**, 1973 (1924).

(31) E. J. Bowen and W. S. Metcalf, *Proc. R. Soc. London, Ser. A*, **206**, 937 (1951).

(32) W. R. Ware, "Creation and Detection of the Excited State", Vol. 1A, A. A. Lamola, Ed., Marcel Dekker, New York, N.Y., 1971, p 213.

(33) J. Saltiel, D. E. Townsend, B. D. Watson, and P. Shannon, *J. Am. Chem. Soc.*, **97**, 5688 (1975).

(34) P. J. Wagner and I. Kochevar, *J. Am. Chem. Soc.*, **90**, 2232 (1968).

(35) At the higher DMA concentrations, especially in the presence of air some of the curvature may be due to internal filtering of the excitation light by DMA (see UV data in Results section). Use of the active sphere model gives 7.05 Å as the radius of the active sphere.

(36) Previous measurements of τ_m^0 in dilute benzene solution have yielded values of 4.2, 4.0,[14,38] and 4.26[39] ns in good agreement with our work. These lifetimes are all significantly shorter than values obtained in saturated hydrocarbon solvents, e.g., τ_m^0 = 5.6 ns in degassed cyclohexane,[40] 25 °C, and may be more appropriately associated with the decay of an anthracene/benzene exciplex.

(37) W. R. Ware, *J. Phys. Chem.*, **66**, 455 (1962).

(38) W. S. Metcalf, *J. Sci. Instrum.*, **42**, 603 (1965).

(39) W. R. Ware and B. A. Baldwin, *J. Chem. Phys.*, **40**, 1703 (1964).

(40) B. D. Watson, P. Shannon, D. E. Townsend, and J. Saltiel, unpublished observations.

(41) H. Beens and A. Weller, *Chem. Phys. Lett.*, **2**, 140 (1968).

(42) Reference 7, p 445.

(43) G. N. Taylor, E. A. Chandross, and A. H. Schiebel, *J. Am. Chem. Soc.*, **96**, 2693 (1974).

(44) Quenching of exciplex emission by third molecules not involved in the formation of the exciplex has also been reported.[33,45]

(45) D. Creed and R. A. Caldwell, *J. Am. Chem. Soc.*, **96**, 7369 (1974).

(46) K. H. Grellmann and U. Suckow, *Chem. Phys. Lett.*, **32**, 250 (1975).

(47) Cf., also, ref 46, where evidence is presented suggesting reversibility in triplex formation.

(48) J. Saltiel et al., *Pure Appl. Chem.*, **41**, 559 (1975).

(49) For the mechanism of quenching of aromatic hydrocarbon singlets by oxygen see B. Stevens, *Acc. Chem. Res.*, **6**, 90 (1973) and L. K. Patterson, G. Porter, and M. R. Topp, *Chem. Phys. Lett.*, **7**, 612 (1970).

(50) D. F. Evans, *J. Chem. Soc.*, 345 (1953); cf. also, H. Tsubomura and R. S. Mulliken, *J. Am. Chem. Soc.*, **82**, 5966 (1960).

(51) M. Suzuki, *Bull. Chem. Soc. Jpn.*, **18**, 146 (1943).

(52) M. Suzuki, *Bull. Chem. Soc. Jpn.*, **22**, 172 (1949).

(53) M. Suzuki, *Bull. Chem. Soc. Jpn.*, **23**, 120 (1950).

(54) E. J. Bowen, *Adv. Photochem.*, **1**, 23 (1963).

(55) B. Stevens, T. Dickinson, and R. R. Sharpe, *Nature (London)*, **204**, 876 (1964).

(56) B. Stevens, R. R. Sharpe, and S. A. Emmons, *Photochem. Photobiol.*, **4**, 603 (1965).

(57) Cf., however, R. L. Barnes and J. B. Birks, *Proc. R. Soc. London, Ser. A*, **291**, 570 (1966), where these are suggested to be competitive processes.

(58) E. J. Bowen and D. W. Tanner, *Trans. Faraday Soc.*, **51**, 475 (1955).
(59) The biacetyl-sensitized photodimerization of anthracene has been reported,[60] as well as the strong self-quenching of anthracene triplets.[61]
(60) H. L. J. Bäckström and K. Sandros, *Acta Chem. Scand.*, **12**, 823 (1958).
(61) J. Langelaar, G. Jansen, R. P. H. Rettschnick, and G. J. Hoytink, *Chem. Phys. Lett.*, **12**, 86 (1971).
(62) E. J. Bowen, *Trans. Faraday Soc.*, **50**, 97 (1954).
(63) We thank Professor B. Stevens for informing us that the "ordinary temperature" in Bowen's laboratory was ~15 °C.
(64) E. A. Chandross, J. Ferguson, and E. G. McRae, *J. Chem. Phys.*, **45**, 3546 (1966).
(65) J. Ferguson and A. W.-H. Mau, *Mol. Phys.*, **27**, 377 (1974).
(66) T. Vember, T. V. Veselova, I. E. Obyknovennaya, A. Cherkasov, and V. Shirokov, *Izv. Akad. Nauk. SSSR, Ser. Fiz.*, **37**, 837 (1973).
(67) M. D. Cohen, A. Ludmer, and V. Yakhot, *Chem. Phys. Lett.*, **38**, 398 (1976).
(68) A kinetic analysis of the photooxidation data in ref 58 using Stevens' mechanism for self-peroxidation[49] shows the photooxidation data in the presence of air to be consistent with those in the presence of pure oxygen.
(69) N. A. Lange, "Handbook of Chemistry", 9th ed., Handbook Publishers, Sandusky, Ohio, 1956, p 1658.
(70) K. S. Wei and R. Livingston, *Photochem. Photobiol.*, **6**, 229 (1967).
(71) If the lines in Figure 10 are drawn so that the intercept/slope ratios equal the spectroscopically determined value of ~1.20, then $k_{eox}'[O_2] = 0.24$ and $\tau_e^{0\prime} = 6$ ns are obtained.
(72) H. Ohta, D. Creed, P. H. Wine, R. A. Caldwell, and L. A. Melton, *J. Am. Chem. Soc.*, **98**, 2002 (1976).
(73) At higher [A] anthracene loss quantum yields were also obtained in the presence of 0.039 M DMA using procedure 1 and anthracene dimerization (no DMA) as the actinometer. At 0.056 and 0.074 M [A], ϕ_{-A} values of 0.235 and 0.310 were measured, respectively, at 30 °C.
(74) N. C. Yang, D. M. Shold, and B. Kim, *J. Am. Chem. Soc.*, **98**, 6587 (1976). We thank Professor N. C. Yang for a preprint of this manuscript.
(75) J. Saltiel, H. C. Curtis, and B. Jones, *Mol. Photochem.*, **2**, 331 (1970).
(76) F. G. Moses, R. S. H. Liu, and B. M. Monroe, *Mol. Photochem.*, **1**, 245 (1969).
(77) J. Saltiel and E. D. Megarity, *J. Am. Chem. Soc.*, **94**, 2742 (1972).

Photochemical Substitution Reactions of Group 6B Metal Tetracarbonyl Norbornadiene Complexes with ^{13}CO, Kinetics of Subsequent Thermal Rearrangements in the Stereospecifically Labeled Species, and Relationship of These Results to the Photoinduced Hydrogenation Process

Donald J. Darensbourg,* Herbert H. Nelson, III, and Mark A. Murphy

Contribution from the Department of Chemistry, Tulane University, New Orleans, Louisiana 70118. *Received July 26, 1976*

Abstract: Photochemical substitution reaction ($\lambda > 2800$ Å) of $M(CO)_4(NBD)$ (M = Cr, Mo, W and NBD = norbornadiene) with ^{13}CO have been shown via infrared spectroscopy, coupled with ^{13}C NMR, to occur with preferential loss of an axial CO ligand. Further rearrangement of the stereospecifically ^{13}CO labeled $M(CO)_4(NBD)$ species results upon thermal and/or photochemical activation. A mechanism for this rearrangement in the tungsten derivative has been proposed based on kinetic measurements (both for the rearrangement process and diolefin substitution with phosphines) which involves cleavage of one metal–olefin bond, followed by a Berry permutation. The results of thermal and photochemical hydrogenation of norbornadiene in the presence of group 6b hexacarbonyls are explained employing CO dissociation as well as metal–olefin bond cleavage.

Introduction

Several studies on photoinduced hydrogenation of conjugated dienes in the presence of chromium carbonyl complexes have been published in recent years.[1-4] Chromium tetracarbonyl norbornadiene has been implicated as an intermediate in the photoassisted hydrogenation[2] and dimerization[5] of norbornadiene with chromium hexacarbonyl. Although metal carbonyl derivatives have been demonstrated to readily lose carbonyl ligands upon photolysis,[6-8] Platbrood and Wilputte-Steinert have concluded, based on an extensive mechanistic investigation of the photoinduced hydrogenation of (norbornadiene)$Cr(CO)_4$, that the primary photochemical process in these reactions involves a metal–olefin bond rupture.[2] Similarly, thermal hydrogenation of 1,3-dienes involving chromium carbonyl complexes as catalysts have been investigated,[9,10] and Schroeder and Wrighton[10] have proposed that these reactions proceed through an intermediate common with that of the photocatalyzed process, (diene)$Cr(CO)_3H_2$. During this time we published our initial investigation of photochemical substitution reactions of group 6b metal tetracarbonyl norbornadiene with ^{13}CO which indicated that these species were rapidly enriched with ^{13}CO.[11] Recently, Platbrood and Wilputte-Steinert[12] have as well shown that photochemical reaction of (norbornadiene)$Cr(CO)_4$ with triphenylphosphine leads to the production of *mer*-(norbornadiene)$Cr(CO)_3P(C_6H_5)_3$ which was in agreement with earlier, less definitive work of King and Korenowski[13] on photochemical reactions of (norbornadiene)$W(CO)_4$ with $As(C_6H_5)_3$ and $Sb(C_6H_5)_3$. These workers[12] also observed that the rate of $P(C_6H_5)_3$ substitution into (norbornadiene)$Cr(CO)_4$ and the rate of hydrogenation of (norbornadiene)$Cr(CO)_4$ were similar, thus indicating that CO dissociation is possibly the rate-determining step in the hydrogenation process.

In addition to the interest in (norbornadiene)$M(CO)_4$ derivatives as catalysts in the photochemical hydrogenation process of norbornadiene, a model system for the general diene photoinduced hydrogenation in the presence of hexacarbonyls, we have been interested in the stereospecificity of photochemical substitution reactions of substituted metal carbonyl derivatives in general.[14,15] For these reasons we have examined the stereoselectivity of group 6b metal tetracarbonyl norbornadiene species toward photochemical substitution processes with ^{13}CO as well as subsequent thermal rearrangements of some of the ^{13}CO substituted species. This report represents a detailed presentation of our earlier communication,[11] as well